

On the static and small signal analysis of DAB converter

Yuxin Yang Hang Zhou Hourong Song Branislav Hredzak

Abstract—This document develops a method to solve the periodic operating point of Dual-Active-Bridge (DAB).

Index Terms—modal analysis, power electronics, Control theory.

I. INTRODUCTION

THE Dual-Active-Bridge is widely used for DC nano grid. In order to optimize the parameter design, a conversion ratio and a modal analysis are required. The traditional voltage & second balancing method is not applicable. Discrete time modeling method has been utilized to model the stability [1][2]. However, the complexity of existing discrete time model of DAB converter is too high for practical use. This paper derive a simplified discrete time model without sacrificing the accuracy. Therefore it is more practical for engineering use.

II. PROBLEM STATEMENT AND OBJECTIVES

We consider a piecewise linear time-invariant system over one period T_s , divided into n consecutive intervals of durations T_1, \dots, T_n (with $T_s = \sum_{i=1}^n T_i$). On interval i the system is governed by

$$\dot{\mathbf{X}}(t) = A_i \mathbf{X}(t) + B_i \mathbf{U},$$

where the input \mathbf{U} is held constant in each interval. Denote the state at the start of the i th interval by \mathbf{X}_{i-1} , then the discrete-time update is

$$\begin{aligned} \mathbf{X}_i &= \Phi_i \mathbf{X}_{i-1} + \Gamma_i, \quad \Phi_i = e^{A_i T_i}, \\ \Gamma_i &= \int_0^{T_i} e^{A_i(T_i-\tau)} B_i \mathbf{U} d\tau. \end{aligned} \quad (1)$$

Our goal is to derive:

- 1) A closed-form expression for \mathbf{X}_n in terms of \mathbf{X}_0 and the Γ_i .
- 2) The fixed-point equation for the periodic steady state \mathbf{X}^* satisfying $\mathbf{X}_n = \mathbf{X}_0 = \mathbf{X}^*$.

III. PRODUCT NOTATION: DIRECTION AND BOUNDARY

We introduce two notations for multiplying the transition matrices:

$$\prod_{j=a}^b \Phi_j := \Phi_a \Phi_{a+1} \cdots \Phi_b, \quad \prod_{j=a}^b \Phi_j := \Phi_b \Phi_{b-1} \cdots \Phi_a,$$

for $a \leq b$. In particular,

$$\prod_{j=a}^a \Phi_j = \prod_{j=a}^a \Phi_j = \Phi_a.$$

In our closed-form formula only the “reverse” product $\prod_{j=1}^n \Phi_j$ appears, avoiding any need for an empty-product convention.

IV. MAIN RESULTS: RECURSIVE CLOSED-FORM AND FIXED-POINT EQUATION

A. Recursive Closed-Form

For any $n \geq 1$, the state at the end of the n th interval is

$$\mathbf{X}_n = \left(\prod_{j=1}^n \Phi_j \right) \mathbf{X}_0 + \sum_{i=1}^{n-1} \left(\prod_{j=i+1}^n \Phi_j \right) \Gamma_i + \Gamma_n \quad (1)$$

B. Periodic Fixed-Point Equation

If a periodic steady state $\mathbf{X}^* = \mathbf{X}_0 = \mathbf{X}_n$ exists, it satisfies

$$(I - \Pi) \mathbf{X}^* = \sum_{i=1}^{n-1} \left(\prod_{j=i+1}^n \Phi_j \right) \Gamma_i + \Gamma_n, \quad \Pi := \prod_{j=1}^n \Phi_j. \quad (2)$$

Take four state transition as an example:

$$\begin{aligned} X_1 &= \Phi_1 X_0 + \Gamma_1, \\ X_2 &= \Phi_2 \Phi_1 X_0 + \Phi_2 \Gamma_1 + \Gamma_2, \\ X_3 &= \Phi_3 \Phi_2 \Phi_1 X_0 + \Phi_3 \Phi_2 \Gamma_1 + \Phi_3 \Gamma_2 + \Gamma_3, \\ X_4 &= \Phi_4 \Phi_3 \Phi_2 \Phi_1 X_0 + \Phi_4 \Phi_3 \Phi_2 \Gamma_1 + \Phi_4 \Phi_3 \Gamma_2 + \Phi_4 \Gamma_3 + \Gamma_4. \end{aligned} \quad (2)$$

V. SYSTEM MATRICES FOR DUAL ACTIVE BRIDGE

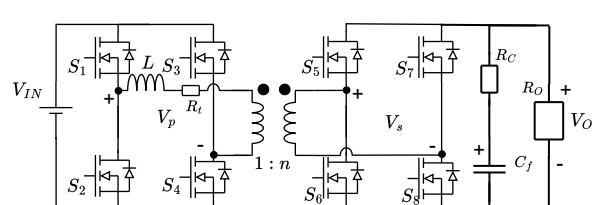


Fig. 1: Schematic of the DAB converter

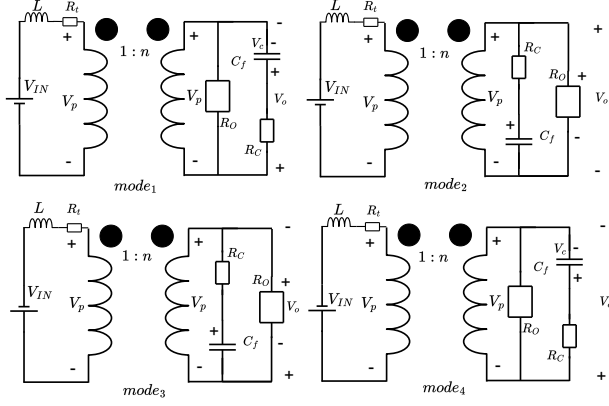


Fig. 2: Schematic of the piecewise intervals.

- 1) Subinterval T_1 : S_1, S_4, S_6, S_7 are ON; S_2, S_3, S_5, S_8 are OFF (A_1, B_1, C_1).
- 2) Subinterval T_2 : S_1, S_4, S_5, S_8 are ON; S_2, S_3, S_6, S_7 are OFF (A_2, B_2, C_2).
- 3) Subinterval T_3 : S_2, S_3, S_5, S_8 are ON; S_1, S_4, S_6, S_7 are OFF.
- 4) Subinterval T_4 : S_2, S_3, S_6, S_7 are ON; S_1, S_4, S_5, S_8 are OFF.

$$X = \begin{bmatrix} i_L \\ v_{CO} \end{bmatrix} \quad Y = [v_O] \quad U = [V_{IN}] \quad (3)$$

The output variable is :

$$\mathbf{y} = \begin{bmatrix} I_{rec} \\ V_{out} \end{bmatrix}$$

All matrices refer to the four-interval model ($n = 4$):

$$A_1 = A_4 = \begin{bmatrix} \frac{n^2 R_t + \frac{R_o R_C}{R_o + R_C}}{n^2 L} & \frac{R_o}{n L (R_o + R_C)} \\ -\frac{R_o}{n C_o (R_o + R_C)} & -\frac{1}{C_o (R_o + R_C)} \end{bmatrix}$$

$$A_2 = A_3 = \begin{bmatrix} \frac{n^2 R_t + \frac{R_o R_C}{R_o + R_C}}{n^2 L} & -\frac{R_o}{n L (R_o + R_C)} \\ \frac{R_o}{n C_o (R_o + R_C)} & -\frac{1}{C_o (R_o + R_C)} \end{bmatrix}$$

$$B_1 = B_2, \quad B_3 = B_4$$

$$B_1 = B_2 = \begin{bmatrix} \frac{1}{L} \\ 0 \end{bmatrix}, \quad B_3 = B_4 = \begin{bmatrix} -\frac{1}{L} \\ 0 \end{bmatrix}.$$

$$C_1 = \begin{bmatrix} -\frac{1}{n} & 0 \\ -\frac{1}{n} (R_C \parallel R_o) & \frac{R_o}{R_C + R_o} \end{bmatrix},$$

$$C_2 = \begin{bmatrix} \frac{1}{n} & 0 \\ \frac{1}{n} (R_C \parallel R_o) & \frac{R_o}{R_C + R_o} \end{bmatrix},$$

$$C_3 = C_2,$$

$$C_4 = C_1,$$

VI. NOTATION

$$S = \text{diag}(1, -1), \quad D' = \text{diag}(-1, 1), \quad SD' = -I.$$

For each subinterval $i = 1, \dots, 4$ let

$$\Phi_i = e^{A_i T_i}, \quad \Gamma_i = A_i^{-1} (\Phi_i - I) B_i U.$$

VII. SIMILARITY / SIGN IDENTITIES

$$\begin{aligned} A_2 &= A_3 = S A_1 S, & A_4 &= A_1, \\ B_1 &= B_2, & B_3 &= B_4 = -B_1, \\ T_1 &= T_3, & T_2 &= T_4. \end{aligned}$$

Lemma 1 (Similarity and Sign Relations). *Let*

$$\Phi_i = e^{A_i T_i}, \quad \Gamma_i = A_i^{-1} (\Phi_i - I) B_i U, \quad S = \text{diag}(1, -1),$$

with the structural and timing assumptions

$$\begin{aligned} A_2 &= A_3 = S A_1 S, & A_4 &= A_1, \\ B_1 &= B_2, \quad B_3 = B_4 = -B_1, & T_1 &= T_3, \quad T_2 = T_4. \end{aligned}$$

Then the following hold:

$$\Phi_3 = S \Phi_1 S, \quad \Phi_4 = S \Phi_2 S, \quad \Gamma_3 = -S \Gamma_1, \quad \Gamma_4 = -S \Gamma_2.$$

Proof. We verify each identity in turn, keeping every factor of S explicit.

1. $\Phi_3 = S \Phi_1 S$.

$$\begin{aligned} \Phi_3 &= e^{A_3 T_3} = e^{(S A_1 S) T_1} = S e^{A_1 T_1} S \\ &= S \Phi_1 S. \end{aligned} \quad (4)$$

2. $\Phi_4 = S \Phi_2 S$.

$$\Phi_4 = e^{A_4 T_4} = e^{A_1 T_2} = S e^{A_1 T_2} S = S \Phi_2 S. \quad (5)$$

3. $\Gamma_3 = -S \Gamma_1$.

$$\begin{aligned} \Gamma_3 &= A_3^{-1} (\Phi_3 - I) B_3 U \\ &= (S A_1 S)^{-1} (S \Phi_1 S - I) (-B_1) U \\ &= S A_1^{-1} S [S (\Phi_1 - I) S] (-B_1) U \\ &= -S [A_1^{-1} (\Phi_1 - I) B_1 U] = -S \Gamma_1. \end{aligned} \quad (6)$$

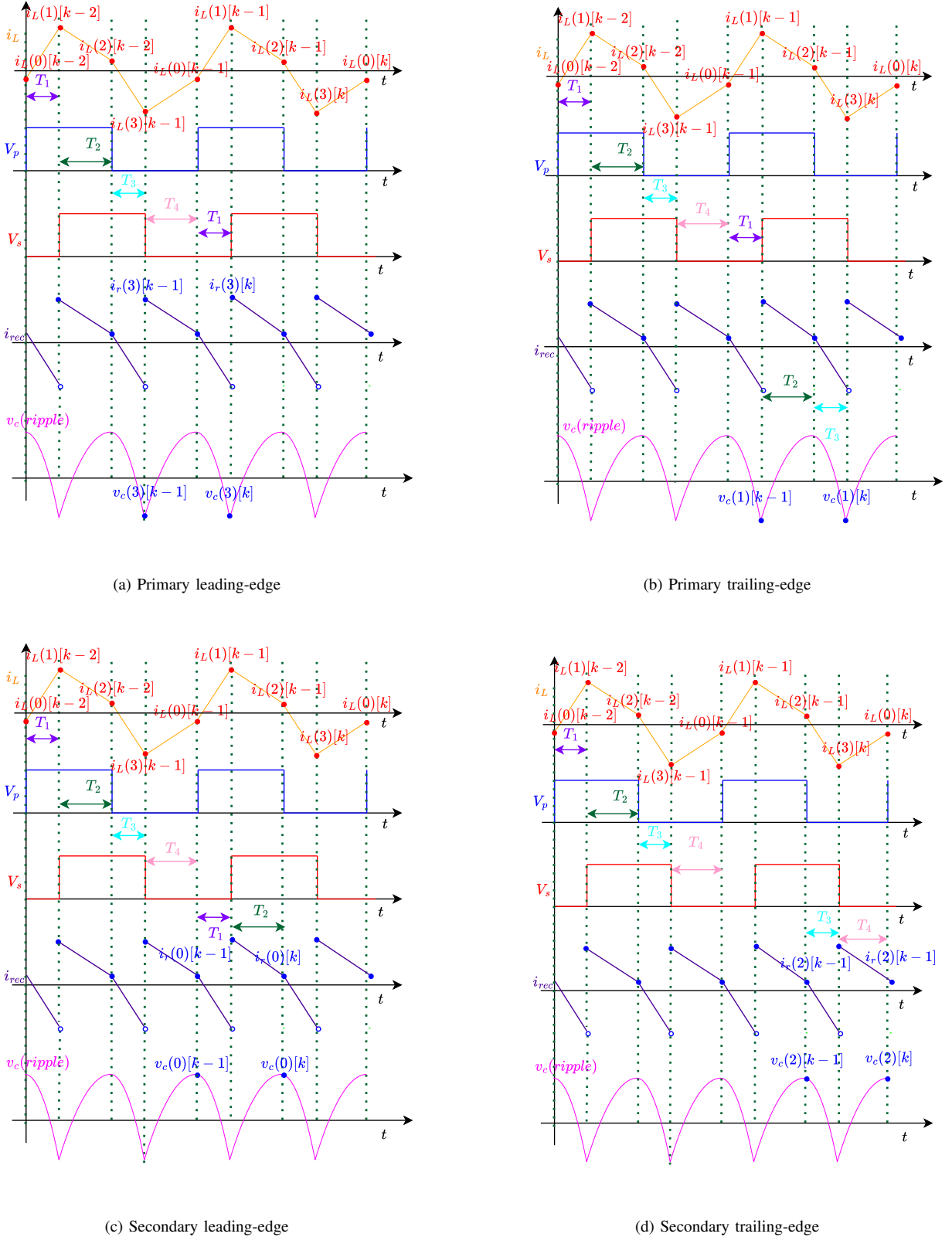


Fig. 3: Four modulation edges in DAB control.

$$4. \Gamma_4 = -S\Gamma_2.$$

$$\begin{aligned}
 \Gamma_4 &= A_4^{-1}(\Phi_4 - I)B_4U \\
 &= A_1^{-1}(\Phi_4 - I)(-B_1)U \\
 &= -A_1^{-1}(S\Phi_2S - I)B_1U \\
 &= -A_1^{-1}S(\Phi_2 - I)SB_1U
 \end{aligned} \tag{7}$$

This completes the proof of all four identities. \blacksquare

VIII. H - G OPERATOR PROOF FOR THE FOUR-STEP FIXED POINT

Theorem 2 (Half-Cycle Fixed-Point Characterization). *Under the symmetry assumptions*

$$S = \text{diag}(1, -1), \quad D' = \text{diag}(-1, 1),$$

$$SD' = -I, \quad T_1 = T_3, \quad T_2 = T_4,$$

$$A_2 = A_3 = SA_1S,$$

$$A_4 = A_1, \quad B_3 = B_4 = -B_1,$$

let

$$\Phi_i = e^{A_i T_i}, \quad \Gamma_i = \int_0^{T_i} e^{A_i(T_i - \tau)} B_i U d\tau,$$

and define the half-cycle map

$$H(X) = \Phi_2 \Phi_1 X + (\Phi_2 \Gamma_1 + \Gamma_2).$$

Then the full-period fixed-point condition

$$\begin{aligned} X_4 &= \Phi_4 \Phi_3 \Phi_2 \Phi_1 X_0 + \Phi_4 \Phi_3 \Phi_2 \Gamma_1 \\ &\quad + \Phi_4 \Phi_3 \Gamma_2 + \Phi_4 \Gamma_3 + \Gamma_4 = X_0 \end{aligned} \quad (8)$$

is equivalent to the much shorter “half-cycle” condition

$$H(X_0) = D' X_0.$$

In other words, verifying

$$\Phi_2 \Phi_1 X_0 + (\Phi_2 \Gamma_1 + \Gamma_2) = D' X_0$$

alone guarantees $X_4 = X_0$, thereby reducing the four-step iteration to a two-step check.

Proof. Step1: Define Two Half-Cycle Maps

$$H(X) = \Phi_2 \Phi_1 X + \Phi_2 \Gamma_1 + \Gamma_2,$$

$$G(Z) = \Phi_4 \Phi_3 Z + \Phi_4 \Gamma_3 + \Gamma_4.$$

Step2: Two-Step Flip Condition

$$H(X_0) = D' X_0. \quad (\text{H})$$

Step3: Structure of G

$$G(Z) = S \left[\Phi_2 \Phi_1 (SZ) - \Phi_2 \Gamma_1 - \Gamma_2 \right]. \quad (9)$$

Step4: Evaluate G at $Z = H(X_0)$

Because $SD' = -I$,

$$S H(X_0) = -X_0.$$

Insert into (9):

$$\begin{aligned} G(H(X_0)) &= S \left[\Phi_2 \Phi_1 (-X_0) - \Phi_2 \Gamma_1 - \Gamma_2 \right] \\ &= -S \left[\Phi_2 \Phi_1 X_0 + \Phi_2 \Gamma_1 + \Gamma_2 \right]. \end{aligned} \quad (10)$$

Step5: Apply Two-Step Condition Using (H),

$$\Phi_2 \Phi_1 X_0 + \Phi_2 \Gamma_1 + \Gamma_2 = D' X_0.$$

Substitute into (10):

$$G(H(X_0)) = -S D' X_0 = X_0.$$

Step6: Four-Step Closure Since $X_2 = H(X_0)$,

$$X_4 = G(X_2) = G(H(X_0)) = X_0.$$

IX. SMALL-SIGNAL MODEL OF DAB UNDER FIXED-FREQUENCY PHASE MODULATION

A. Notation, rectified half-cycle state, and SIMO physical output

We consider the four-subinterval DAB model over one switching period T_s , and define the half-cycle length $T_h := T_s/2$. The state is

$$\mathbf{x}(t) = \begin{bmatrix} i_L(t) \\ v_C(t) \end{bmatrix}. \quad (11)$$

On subinterval $i \in \{1, 2, 3, 4\}$, the dynamics are

$$\dot{\mathbf{x}}(t) = A_i \mathbf{x}(t) + B_i U, \quad (12)$$

where U is constant over each subinterval.

1) *A. Rectified half-cycle coordinate*: To make the sampled inductor-current sign-consistent across half-cycles, we use the fixed involution

$$D_r := \text{diag}(-1, 1), \quad D_r^{-1} = D_r. \quad (13)$$

All half-cycle maps below are written in this rectified coordinate.

2) *B. Exact segment maps*: For subinterval i with duration T_i , define the exact segment map

$$x^+ = \Phi_i x^- + \Gamma_i, \quad \Phi_i := e^{A_i T_i}, \quad \Gamma_i := \int_0^{T_i} e^{A_i(T_i - \tau)} B_i U d\tau. \quad (14)$$

3) *C. SIMO physical output matrix*: We adopt the SIMO physical output

$$y_k = \begin{bmatrix} I_{\text{rec},k} \\ V_{\text{out},k} \end{bmatrix} = C_{\text{phys}} x_k, \quad (15)$$

where C_{phys} absorbs the turns ratio and the output definition, so no selection matrix is needed:

$$C_{\text{phys}} := \begin{bmatrix} \frac{1}{n} & 0 \\ \frac{R_c \| R_o}{n} & \frac{R_o}{R_c + R_o} \end{bmatrix}, \quad R_c \parallel R_o := \frac{R_c R_o}{R_c + R_o}. \quad (16)$$

Importantly, C_{phys} is the same physical mapping from (i_L, v_C) to $(I_{\text{rec}}, V_{\text{out}})$ on every sampling surface.

B. DAB symmetry identities

Let $S := \text{diag}(1, -1)$ so that

$$D_r = -S. \quad (17)$$

Under the four-interval DAB structure (matched half-cycles), we use

$$\begin{aligned} A_4 &= A_1, & A_2 &= A_3 = SA_1S, \\ B_1 &= B_2, & B_3 &= B_4 = -B_1, \\ T_1 &= T_3, & T_2 &= T_4. \end{aligned} \quad (18)$$

Consequently, the state-transition matrices satisfy

$$\Phi_3 = D_r \Phi_1 D_r, \quad \Phi_4 = D_r \Phi_2 D_r. \quad (19)$$

C. Two-interval rectified half-cycle map on an arbitrary surface

Pick any half-cycle sampling surface such that the half-cycle evolution consists of two consecutive subintervals $a \rightarrow b$ with durations T_a and T_b satisfying

$$T_a + T_b = T_h. \quad (20)$$

1) A. Large-signal half-cycle map: The rectified half-cycle map is

$$\begin{aligned} x_{k+1} &= D_r \left(\Phi_b (\Phi_a x_k + \Gamma_a) + \Gamma_b \right) \\ &=: \Phi^{(ab)} x_k + g^{(ab)}, \end{aligned} \quad (21)$$

where

$$\Phi^{(ab)} := D_r \Phi_b \Phi_a, \quad g^{(ab)} := D_r (\Phi_b \Gamma_a + \Gamma_b). \quad (22)$$

2) B. Endpoint timing sensitivities: Let x^* be the fixed point of (21), and define the intermediate steady states

$$\begin{aligned} x_{a,\text{end}}^* &= \Phi_a x^* + \Gamma_a, \\ x_{b,\text{end}}^* &= \Phi_b x_{a,\text{end}}^* + \Gamma_b. \end{aligned} \quad (23)$$

Using the endpoint vector-field identity, the duration sensitivities are

$$\begin{aligned} \eta_a^{(ab)} &:= \frac{\partial x_{k+1}}{\partial T_a} \Big|_* = D_r \Phi_b \left(A_a x_{a,\text{end}}^* + B_a U \right), \\ \eta_b^{(ab)} &:= \frac{\partial x_{k+1}}{\partial T_b} \Big|_* = D_r \left(A_b x_{b,\text{end}}^* + B_b U \right). \end{aligned} \quad (24)$$

D. Fixed-frequency modulation: correct two-cycle timing split

A fixed-frequency phase modulator anchors one endpoint to the clock and generates the other endpoint by a comparator against a ramp of amplitude V_r . Define the ramp slope magnitude and its reciprocal as

$$|S_e| = \frac{V_r}{T_h}, \quad \kappa := \frac{1}{|S_e|} = \frac{T_h}{V_r}. \quad (25)$$

1) A. Timing law and polarity (primary vs. secondary): Because the half-cycle partition satisfies $T_a + T_b = T_h$, the two adjacent timing perturbations are always opposite in sign. We write the fixed-frequency two-cycle timing law as

$$\hat{T}_{a,k} = \rho \kappa \hat{v}_{c,k}, \quad \hat{T}_{b,k} = -\rho \kappa \hat{v}_{c,k+1}, \quad (26)$$

where $\rho \in \{+1, -1\}$ captures the modulator logic:

$$\rho = \begin{cases} +1, & \text{secondary-side phase modulation (pos logic),} \\ -1, & \text{primary-side phase modulation (neg logic).} \end{cases} \quad (27)$$

2) B. Linearized half-cycle map: Linearizing (21) and substituting (26) yield

$$\hat{x}_{k+1} = \Phi^{(ab)} \hat{x}_k + \beta_-^{(ab)} \hat{v}_{c,k} + \beta_+^{(ab)} \hat{v}_{c,k+1}, \quad (28)$$

where we absorb κ into the two vectors

$$\beta_-^{(ab)} := \rho \kappa \eta_a^{(ab)}, \quad \beta_+^{(ab)} := -\rho \kappa \eta_b^{(ab)}. \quad (29)$$

3) C. SIMO z-domain transfer function: Taking the z transform of (28) gives

$$\hat{X}(z) = (zI - \Phi^{(ab)})^{-1} (\beta_-^{(ab)} + z\beta_+^{(ab)}) \hat{V}_c(z). \quad (30)$$

Therefore, the SIMO transfer from \hat{v}_c to $y = [I_{\text{rec}}, V_{\text{out}}]^T$ is

$$H_{\text{fix}}^{(ab)}(z) = C_{\text{phys}} (zI - \Phi^{(ab)})^{-1} (\beta_-^{(ab)} + z\beta_+^{(ab)}). \quad (31)$$

E. Four sampling surfaces and their transfer functions

The four-interval DAB admits four natural half-cycle sampling surfaces:

$$\begin{aligned} P^+ : (a,b) &= (1,2), & S^+ : (a,b) &= (2,3), \\ P^- : (a,b) &= (3,4), & S^- : (a,b) &= (4,1). \end{aligned} \quad (32)$$

Each surface yields (31), with the corresponding $\Phi^{(ab)}$, $\eta_a^{(ab)}$, $\eta_b^{(ab)}$, and polarity ρ given by (27).

F. Primary-side and secondary-side equivalence via similarity

This subsection formalizes the key fact you validated: even with a single physical C_{phys} , the primary-side and secondary-side realizations are related by a similarity map between *surface states*. Hence they represent the same physical input-output transfer.

1) A. A similarity identity for resolvents:

Lemma 3. *Let T be nonsingular. For any square matrix A ,*

$$(zI - T^{-1}AT)^{-1} = T^{-1}(zI - A)^{-1}T. \quad (33)$$

2) B. Key similarity: $\Phi^{(12)}$ and $\Phi^{(23)}$: Using (19),

$$\Phi^{(23)} = D_r \Phi_3 \Phi_2 = D_r (D_r \Phi_1 D_r) \Phi_2 = \Phi_1 D_r \Phi_2, \quad (34)$$

and

$$\Phi^{(12)} = D_r \Phi_2 \Phi_1. \quad (35)$$

Choose the similarity transform

$$T := \Phi_1. \quad (36)$$

Then

$$\begin{aligned} T^{-1} \Phi^{(23)} T &= \Phi_1^{-1} (\Phi_1 D_r \Phi_2) \Phi_1 \\ &= (\Phi_1^{-1} \Phi_1) D_r \Phi_2 \Phi_1 \\ &= D_r \Phi_2 \Phi_1 = \Phi^{(12)}. \end{aligned} \quad (37)$$

3) C. Matching the z-weighted input vector with correct polarity: Define the z -weighted input vector

$$b^{(ab)}(z) := \beta_-^{(ab)} + z\beta_+^{(ab)}. \quad (38)$$

For P^+ we use $\rho = -1$; for S^+ we use $\rho = +1$ as in (27). With this primary/secondary polarity distinction, the corresponding z -weighted vectors satisfy the surface-coordinate relation

$$b^{(12)}(z) = T^{-1} b^{(23)}(z), \quad T = \Phi_1. \quad (39)$$

(If one incorrectly uses the same polarity for both sides, a global sign mismatch appears.)

4) *D. Transfer equivalence in a common surface coordinate:* Let $x_k^{(12)}$ denote the surface state on P^+ and $x_k^{(23)}$ the surface state on S^+ . From the surface relation induced by $T = \Phi_1$, we use

$$x_k^{(12)} = T^{-1}x_k^{(23)}. \quad (40)$$

Therefore, the output mapping in the S^+ coordinate becomes

$$y_k = C_{\text{phys}}x_k^{(12)} = C_{\text{phys}}T^{-1}x_k^{(23)}. \quad (41)$$

This is the precise sense in which “a single C_{phys} ” is consistent with similarity between surface states: the physical mapping is the same, but expressing it in a different surface coordinate inserts the T^{-1} factor.

Now start from the P^+ transfer:

$$H_{P^+}(z) = C_{\text{phys}}(zI - \Phi^{(12)})^{-1}b^{(12)}(z). \quad (42)$$

Substitute (37) and (39):

$$\begin{aligned} H_{P^+}(z) &= C_{\text{phys}}\left(zI - T^{-1}\Phi^{(23)}T\right)^{-1}T^{-1}b^{(23)}(z) \\ &= C_{\text{phys}}\left(T^{-1}(zI - \Phi^{(23)})^{-1}T\right)T^{-1}b^{(23)}(z) \quad (43) \\ &= (C_{\text{phys}}T^{-1})(zI - \Phi^{(23)})^{-1}b^{(23)}(z). \end{aligned}$$

By (41), the right-hand side is exactly the S^+ transfer expressed in the S^+ surface coordinate. Hence the two surfaces are physically input–output equivalent.

Applying the same argument to the other pair (34) \leftrightarrow (41) yields the equivalence between P^- and S^- .

G. Strong same-cycle constraint and why it is accurate at most frequency

A common simplification replaces $\hat{v}_{c,k+1}$ by $\hat{v}_{c,k}$ in (28), yielding a single-cycle input model.

1) *A. Strong same-cycle model:* Approximating $\hat{v}_{c,k+1} \approx \hat{v}_{c,k}$ gives

$$\hat{x}_{k+1} = \Phi^{(ab)}\hat{x}_k + \beta_{\text{sc}}^{(ab)}\hat{v}_{c,k}, \quad \beta_{\text{sc}}^{(ab)} := \beta_-^{(ab)} + \beta_+^{(ab)}. \quad (44)$$

Thus

$$H_{\text{sc}}^{(ab)}(z) = C_{\text{phys}}(zI - \Phi^{(ab)})^{-1}\beta_{\text{sc}}^{(ab)}. \quad (45)$$

2) *B. Exact–approximate difference and low-frequency bound:* Subtracting (45) from (31) yields

$$\begin{aligned} \Delta H^{(ab)}(z) &:= H_{\text{fix}}^{(ab)}(z) - H_{\text{sc}}^{(ab)}(z) \\ &= C_{\text{phys}}(zI - \Phi^{(ab)})^{-1}(z - 1)\beta_+^{(ab)}. \quad (46) \end{aligned}$$

For $z = e^{j\omega T_h}$,

$$|z - 1| = 2 \left| \sin\left(\frac{\omega T_h}{2}\right) \right| \leq \omega T_h, \quad \omega T_h \ll 1. \quad (47)$$

If $\Phi^{(ab)}$ is stable and has no eigenvalue close to 1, then $(zI - \Phi^{(ab)})^{-1}$ remains bounded near $z \approx 1$ and (46) implies

$$\|\Delta H^{(ab)}(e^{j\omega T_h})\| = O(\omega T_h), \quad \omega \rightarrow 0. \quad (48)$$

Remark 1. Equation (46) shows the discrepancy is shaped by a discrete-difference factor $(z - 1)$, which explains why the strong same-cycle model can be nearly indistinguishable from the correct fixed-frequency model over a wide band, especially when the rectified half-cycle plant has no marginal pole at $z = 1$.

REFERENCES

- [1] A. Tong, L. Hang, H. S.-H. Chung, and G. Li, “Using sampled-data modeling method to derive equivalent circuit and linearized control method for dual-active-bridge converter,” *IEEE Journal of Emerging and Selected Topics in Power Electronics*, vol. 9, no. 2, pp. 1361–1374, 2021.
- [2] L. Shi, W. Lei, Z. Li, J. Huang, Y. Cui, and Y. Wang, “Bilinear discrete-time modeling and stability analysis of the digitally controlled dual active bridge converter,” *IEEE Transactions on Power Electronics*, vol. 32, no. 11, pp. 8787–8799, 2017.